09

# Laue diffraction of X-ray beams in wedge multilayer structures

© V.I. Punegov

Institute of Physics and Mathematics, Federal Research Center "Komi Scientific Center, the Ural Branch of the Russian Academy of Sciences", Syktyvkar, Russia
E-mail: vpunegov@dm.komisc.ru

*Received September 17, 2025*
*Revised October 13, 2025*
*Accepted October 29, 2025*

Dynamical X-ray scattering in a sectional wedge multilayer structure in the Laue case is examined. New recurrence relations characterizing the diffraction of spatially confined X-ray beams in a periodic gradient system are obtained. The distribution of scattering intensity in reciprocal space is mapped for a W/Si wedge multilayer structure in geometric optics and the Fresnel approximation. It is demonstrated that the calculated $q_x$-sections of maps are the same in geometric optics and the Fresnel approximation, while the $q_z$-sections differ significantly.

**Keywords:** wedge multilayer structure, dynamical Laue diffraction, spatially confined X-ray beams, geometric optics, Fresnel approximation.

DOI: 10.61011/TPL.2026.02.63048.20501

It was demonstrated in [1] that the multilayer Laue lenses proposed in [2] cannot focus synchrotron radiation into a spot several nanometers in size. This contradicts the results of other studies [3,4]. It is also a debated point that the best focusing properties are provided by wedge Laue lenses [5]. The calculation of reciprocal space maps (RSMs) of X-ray scattering intensity distribution for multilayer Laue lenses is a rather complex task (especially for lenses with a wedge distribution of the multilayer system period). Therefore, the first step to finding the solution to this problem is to examine the diffraction for a sectional wedge multilayer structure (MS) with its period varying linearly at each local point throughout the depth of the system (in the horizontal direction along the $x$ axis, Fig. 1) and remaining constant throughout the thickness of the system (in the vertical direction along the $z$ axis).

Rocking curves for a plane X-ray wave incident on a sectional wedge MS in the Laue geometry were studied numerically in [6]. The reflection and transmission coefficient profiles were plotted as a function of the gradient of period variation with depth of the multilayer system along the $x$ axis. However, a plane infinitely wide X-ray wave is a model object. In actual experiments, X-ray beams are bound by slits, collimators, or focusing optics. In addition, the plane X-ray wave model does not allow one to calculate RSMs [7]. Note that Laue diffraction of bounded X-ray beams in a multilayer Mo/Si system with a constant period along the $x$ axis was discussed in [8]. At the same time, the angular distribution of intensity of scattering of bounded X-ray beams in reciprocal space by wedge MSs in the Laue geometry has not been studied yet. Thus, the aim of the present study is to develop a computational algorithm for calculating RSMs for multilayer systems with a gradient of period variation over the structure depth within geometric optics (GO) and the Fresnel approximation (FA).

When radiation passes through a slit or a certain other optical element bounding the wave field front, three transmission functions corresponding to geometric optics, the Fresnel approximation, and the Fraunhofer approximation are distinguished. In GO, diffraction at the slit edges is disregarded; radiation propagates along a straight line without changing direction. Therefore, this transmission function is not applicable to narrow slits. The most complete description of radiation passage through a slit is provided by FA.

In GO, the transmission function (boundary condition for an incident beam) in direct space for a slit with size $w$ takes the form

$$Y(z, l_z^{(in)}) = \begin{cases} 1, & -l_z^{(in)}/2 \le z \le l_z^{(in)}/2, \\ 0, & \text{otherwise}, \end{cases} \quad (1)$$

where $l_z^{(in)}$ is the width of the surface region of a periodic structure irradiated by an incident X-ray wave, which is related to the slit size in the following way: $l_z^{(in)} = w/\cos\theta_B$. Since the Bragg angle is small ($\cos\theta_B \approx 1$) in the case of Laue diffraction by an MS, it is fair to assume that $l_z^{(in)} \approx w$.

The Fourier transform of function (1) is written as

$$\hat{Y}\left(\kappa, l_z^{(in)}\right) = \int_{-\infty}^{+\infty} dx \exp(-i\kappa x) Y\left(z, l_z^{(in)}\right) = \frac{\sin(\kappa l_z^{(in)}/2)}{\kappa/2}. \quad (2)$$

In the Fresnel approximation, the transmission function depends not only on the slit size, but also on distance $L$ from the slit to the entrance surface of the MS:

$$Y(z, l_z^{(in)}, L) = \frac{1}{\sqrt{i\lambda L}} \int_{-l_z^{(in)}/2}^{l_z^{(in)}/2} \exp\left(i\pi \frac{(z'-z)^2}{\lambda L}\right) dz'. \quad (3)$$

The Fourier transform of (3) is written as

$$\hat{Y}(\kappa, l_z^{(in)}, L) = P(\kappa, L)\frac{\sin(\kappa l_z^{(in)}/2)}{\kappa/2}, \qquad (4)$$

where $P(\kappa, L) = \exp\left(-i\lambda\frac{L\kappa^2}{4\pi(\cos\theta_B)^2}\right)$ is the propagator in Fourier space [9] in FA.

The Fraunhofer approximation is a special case of the Fresnel approximation with distance $L$ from the slit to the entrance MS surface being very large. The function of radiation transmission through a slit in FA is written as

$$Y(z, l_z^{(in)}, L) = \frac{1}{\sqrt{i\lambda L}}\left[\frac{\sin\left(\pi z l_z^{(in)}/(\lambda L)\right)}{\pi z/(\lambda L)}\right]. \qquad (5)$$

The Fourier transform of this function corresponds to expression (4).

Figure 1 shows the schematic representation of Laue diffraction of an X-ray beam in a wedge MS. The wedge MS period varies with depth along the $x$ axis. Unfortunately, the equations characterizing Laue diffraction in a system with a constant period are inapplicable to wedge MSs. The wedge MS must be represented as a sectional system consisting of elementary vertical strips. The period in a separate vertical strip within elementary depth $l_p = x_p - x_{p-1}$ is considered to be constant; $p = 1, 2, \ldots, P$ is the strip number. If the MS period for the first strip is $d$, the period for strip number $p$ with mismatch $\Delta d_p$ is written as $d_p = d - \Delta d_p$.

The equations for slowly varying X-ray amplitudes in a periodic structure under diffraction conditions [10,11] may be used to characterize diffraction in a periodic structure. In Fourier space, these equations take the following form

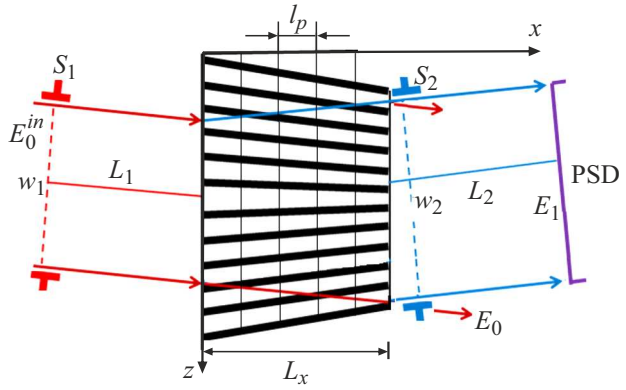


**Figure 1.** Schematic representation of Laue diffraction in a wedge MS with depth $L_x$. $E_{0,1}^{in}$ — amplitude of the incident X-ray wave; $E_{0,1}$ — amplitudes of transmitted and diffraction waves; $w_1$ and $w_2$ — dimensions of incident and diffraction beams, respectively; $L_1$ — distance from slit $S_1$ to the entrance surface of a multilayer structure. Slit $S_2$ is positioned close to the exit MS face. $L_2$ — distance from the exit surface to a position-sensitive detector (PSD).

within the $p$th strip:

$$\begin{cases} \frac{\partial\hat{E}_0^p(\kappa,\eta^p;x)}{\partial x} = i(a_0 - \kappa\tan\theta_B)\hat{E}_0^p(\kappa, \eta^p; x) + ia_1\hat{E}_1^p(\kappa, \eta^p; x), \\ \frac{\partial\hat{E}_1^p(\kappa,\eta^p;x)}{\partial x} = i(a_0 + \eta^p + \kappa\tan\theta_B)\hat{E}_1^p(\kappa, \eta^p; x) + ia_1\hat{E}_0^p(\kappa, \eta^p; x). \end{cases} \qquad (6)$$

Here, $\hat{E}_{0,1}^p(\kappa, \eta; x)$ are the amplitudes of transmitted and diffraction waves, $a_0 = \pi\chi_0/(\lambda\cos\theta_B)$, $a_1 = C\pi\chi_1/(\lambda\cos\theta_B)$, $\lambda$ is the X-ray radiation wavelength in vacuum, and $C$ is the polarization factor. Angle parameter $\eta^p = \eta - h\varepsilon_p^x$ for the $p$th strip is present in system (6). Here, $\eta = 4\pi\sin(\theta_B)\omega/\lambda$, $\omega = \theta - \theta_B$ is the deviation of an incident beam from Bragg angle $\theta_B$, $h = 2\pi/d$, and $\varepsilon_p^x = \Delta d_p\tan\theta_B/d$. The Fourier coefficients of X-ray polarizability in the direction of transmission $\chi_0$ and diffraction $\chi_1$ for an MS with a two-layer period are written as [1]

$$\chi_0 = \frac{\chi_t d_t + \chi_b d_b}{d}, \qquad \chi_1 = \frac{\chi_t - \chi_b}{\pi}\sin\left(\pi\frac{d_t}{d}\right).$$

Here, $\chi_{t,b}$ and $d_{t,b}$ are the Fourier coefficients of polarizabilities and thicknesses of the top $((t))$ and bottom $((b))$ layers of the structure period. X-ray polarizabilities of chemical elements $\chi_j = 2(\delta_j + i\beta_j)$, $j = t, b$, are calculated using tabular values of optical constants $\delta_j = r_0\frac{N_j\lambda^2}{2\pi}(Z_j + \Delta f_j')$, $\beta_j = -r_0\frac{N_j\lambda^2}{2\pi}(\Delta f_j'')$, $r_0 = e^2/mc^2$ is the classical electron radius, $e$, $m$ are the electron charge and mass, $N_j$ is the atomic density, $Z$ is the number of electrons in an atom, and $\Delta f_j'$ are $\Delta f_j''$ are the dispersion corrections to the atomic amplitude.

In the case of spatially restricted beams, Eqs. (6) must be supplemented with boundary conditions. The boundary condition for an incident X-ray beam in Fourier space has the form $\hat{E}_0^1(\kappa, \eta^1; x_1) = \hat{Y}(\kappa, l_z^{(in)}, L_1)$. The second boundary condition is satisfied for a diffraction wave: $\hat{E}_1^1(\kappa, \eta^1; x_1) = 0$. Using the diffraction boundary conditions for each wedge MS strip, we obtain recurrence relations for the X-ray field amplitudes

$$\begin{aligned} \hat{E}_0^{p+1}(\kappa, \eta^p; x_{p+1}) &= \left[B_1^0\exp\left(i\hat{\xi}_1^p l_p\right)\right. \\ &\quad \left. - B_2^0\exp\left(i\hat{\xi}_2^p l_p\right)\right]\hat{Y}(\kappa, l_z^{(in)}, L_1), \\ \hat{E}_1^{p+1}(\kappa, \eta^p; x_{p+1}) &= \left[B_1^1\exp\left(i\hat{\xi}_1^p l_p\right)\right. \\ &\quad \left. - B_2^1\exp\left(i\hat{\xi}_2^p l_p\right)\right]\hat{Y}(\kappa, l_z^{(in)}, L_1), \end{aligned} \qquad (7)$$

where

$$\begin{aligned} B_{1,2}^0 &= \phi_{1,2}^0\hat{E}_0^p(\kappa, \eta^p; x_p) + a_1\hat{E}_1^p(\kappa, \eta^p; x_p)/\hat{\xi}^p, \\ B_{1,2}^1 &= \phi_{1,2}^1\hat{E}_1^p(\kappa, \eta^p; x_p) + a_1\hat{E}_0^p(\kappa, \eta^p; x_p)\hat{\xi}^p, \\ \phi_{1,2}^0 &= (a_0 - \kappa\tan\theta - \hat{\xi}_{2,1}^p)/\hat{\xi}^p, \\ \phi_{1,2}^1 &= (a_0 + \eta^p + \kappa\tan\theta_B - \hat{\xi}_{2,1}^p)/\hat{\xi}^p, \end{aligned}$$

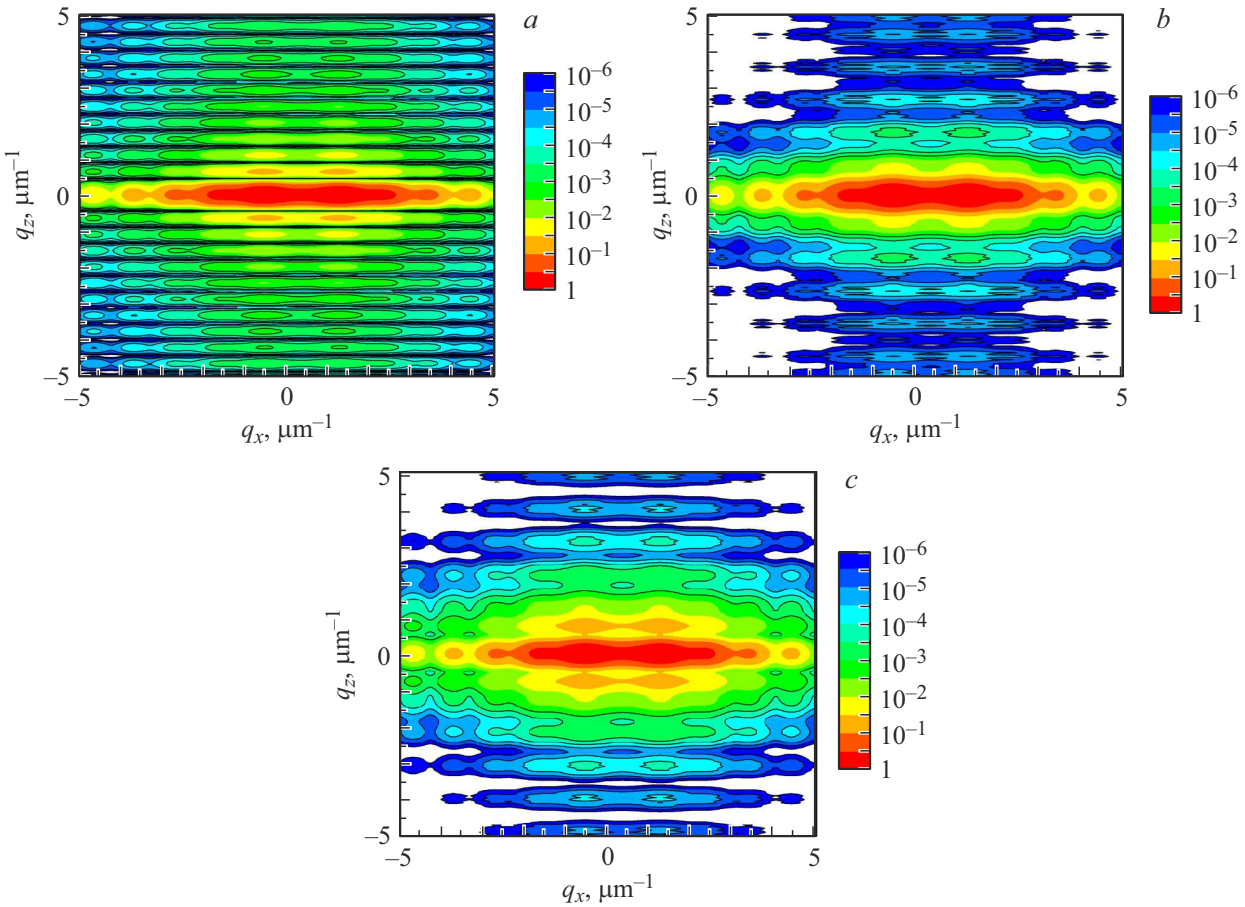


**Figure 2.** Calculated RSMs in logarithmic scale for the wedge W/Si MS, $l_z^{(in)} = 14.0\,\mu$m and $l_z^{(ex)} = 14.2\,\mu$m. *a* — Geometric optics; *b* — Fresnel approximation, the distances from the entrance and exit slits to the detector are the same, $L_1 = L_2 = 2$ m; *c* — Fresnel approximation, $L_1 = L_2 = 0.8$ m.

$$\hat{\xi}^p = \sqrt{(\eta^p + 2\kappa\tan\theta_B)^2 + 4a_1^2},$$

$$\hat{\xi}^p_{1,2} = (2a_0 + \eta^p \pm \hat{\xi}^p)/2.$$

A triple-axis diffraction setup, which is used to measure RSMs, includes a monochromator, the examined sample, and an analyzer (position-sensitive detector). Angular position $\varepsilon$ of the analyzer is written as $\varepsilon = \bar{\omega} + \omega$, where $\bar{\omega}$ is the deviation of the diffracted beam from Bragg angle $\theta_B$ [12]. In the symmetric Laue geometry, angular offsets $\omega$ and $\varepsilon$ are related to the projections of diffraction vector deviation in horizontal $q_x = k\sin\theta_B(2\omega - \varepsilon)$ and vertical $q_z = -k\cos\theta_B\varepsilon$ directions. The angular parameter in reciprocal space is expressed in terms of these projections as $\eta = q_x - q_z\tan\theta_B$. Thus, the solutions for the amplitude of transmitted and diffracted waves take the form

$$E_0(q_x, q_z) = \frac{1}{2\pi}\int_{-\infty}^{+\infty} d\kappa \hat{E}_0^p(\kappa, q_x - q_z\tan\theta_B - h\varepsilon_p^x x_p)$$

$$\times \hat{Y}(\kappa, l_z^{(in)}, L_1)\hat{Y}(\kappa - q_z, l_z^{(ex)}, L_2),$$

$$E_1(q_x, q_z) = \frac{1}{2\pi}\int_{-\infty}^{+\infty} d\kappa \hat{E}_1^p(\kappa, q_x - q_z\tan\theta_B - h\varepsilon_p^x, x_p)$$

$$\times \hat{Y}(\kappa, l_z^{(in)}, L_1)\hat{Y}(\kappa - q_z, l_z^{(ex)}, L_2), \qquad (8)$$

where $\hat{Y}(\kappa - q_z, l_z^{(ex)}, L_2) = P([\kappa - q_z], L_2)\frac{\sin([\kappa - q_z]l_z^{(ex)}/2)}{[\kappa - q_z]/2}$ is the boundary condition for X-ray fields on the exit face and $L_2$ is the distance from slit $S_2$ located close to the side MS surface to the analyzer (position-sensitive detector PSD, Fig. 1).

X-ray reciprocal space maps were modeled for a W/Si MS. In all cases, the intensity of synchrotron radiation incident on the wedge MS was normalized to unity. The size of the multilayer system region irradiated by an incident X-ray beam along the $z$ axis is $w_1 \approx L_z = 14\,\mu$m, and the sectional depth is $L_x = 7\,\mu$m. Numerical calculations were performed for $\sigma$-polarized radiation (polarization factor $C = 1$) with wavelength $\lambda = 0.062$ nm. The W/Si system period is $d = d_W + d_{Si} = 6$ nm, where $d_W = d_{Si} = 3$ nm; Bragg angle $\theta_B = 5.17$ mrad. The optical constants for the MS are $\chi_0 = (-9.35 + i0.68)\cdot 10^{-6}$ and $\chi_1 = (-4.6 + i0.43)\cdot 10^{-6}$. The wedge MS period changes

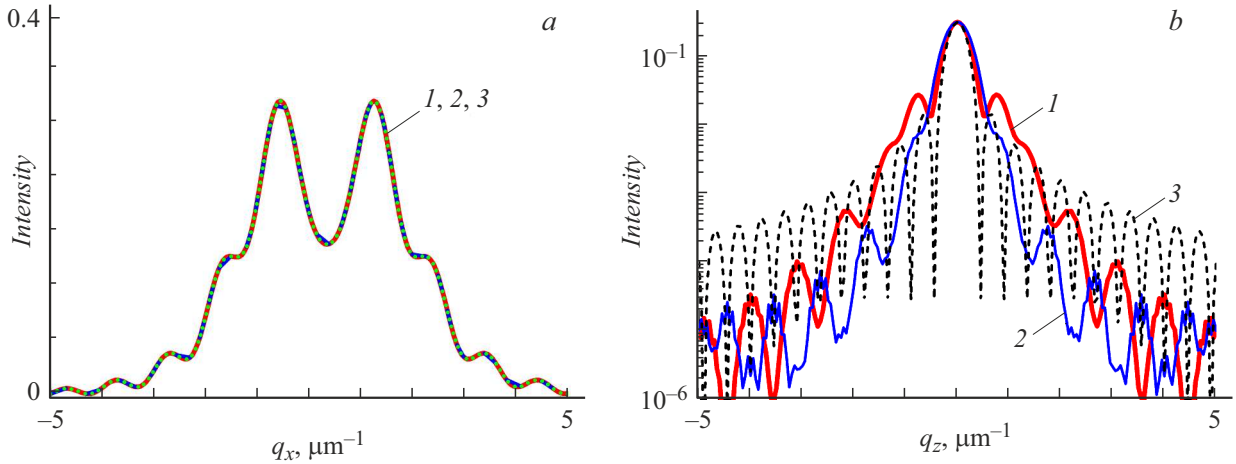


**Figure 3.** Calculated $q_x$-sections ($a$) and $q_z$-sections ($b$) of RSMs of the wedge W/Si MS. *1* — Fresnel approximation, $L_1 = L_2 = 0.8$ m; *2* — Fresnel approximation, $L_1 = L_2 = 2$ m; *3* — geometric optics.

with depth $x$ from 6 to 5.97 nm; the overall period mismatch is 0.03 nm.

Figure 2, $a$ shows the calculated RSM in logarithmic scale for the W/Si wedge multilayer structure in the geometric optics approximation. The dimensions of incident and diffracted beams were the same in calculations both for GO and the Fresnel approximation: $w_1 = w_2 = 14.0\,\mu$m. In GO, the distance from elements limiting the incident beam width to the wedge MS and the distance from elements limiting the diffracted beam width to the detector do not affect the distribution of scattering intensity in reciprocal space. The calculated maps of the X-ray scattering intensity distribution in the Laue geometry in the Fresnel approximation depend on the distances at which the slits bounding the incident and diffracted beams are located. Figure 2, $b$ shows the diffraction pattern calculated in FA; the distance from the entrance slit to the MS is $L_1 = 2$ m. The distance from the exit surface to the detector is the same: $L_2 = 2$ m. Fig. 2, $c$ presents the scattering intensity distribution in reciprocal space at $L_1 = L_2 = 0.8$ m. According to the data in Fig. 2, the contours of equal intensity in the calculated RSMs for geometric optics and different setups in the Fresnel approximation are visually different.

Sections of the calculated RSMs are shown in Fig. 3. The calculated $q_x$-sections (diffraction profiles of the main peaks in the Laue geometry) for GO and different cases in the Fresnel approximation match (Fig. 3, $a$). At the same time, the $q_z$-sections differ significantly (Fig. 3, $b$). Therefore, distortions arising in the structure of an X-ray wavefront in the course of its propagation through slits limiting the transverse dimensions of beams affect the shape of $q_z$-sections of RSMs. A periodic distribution of diffraction intensity is seen in the $q_z$-section profiles. The oscillation periods corresponding to the three examined cases differ. Unfortunately, complex diffraction equations make it impossible to examine the emergence of intensity oscillations analytically (especially within the context of recurrence relations). In the simplest GO case, the period of intensity oscillations of the $q_z$-sections of RSMs is inversely proportional to detector window size $w_2 = l_z^{(ex)} \cos\theta_B$. Note that in the Fresnel approximation, the oscillation period depends not only on $w_2$, but also on distance $L_2$ from the exit MS surface to the detector.

Thus, the developed method may be used for X-ray diffraction Laue diagnostics of arbitrary gradient MSs. It is also applicable to crystals with various lattice deformations (induced, e.g., by elastic bending or a temperature gradient). The method may also find application in studies of layered structures containing low-angle wedges, which are widely used as linear variable filters in microspectrometers, sensors, and hyperspectral imaging systems.

## Funding

This study was carried out under the state assignment of the Institute of Physics and Mathematics of Federal Research Center „Komi Scientific Center, Ural Branch of the Russian Academy of Sciences“ (research project No. 125020501562-1).

## Conflict of interest

The author declares that he has no conflict of interest.

## References

[1] V.I. Punegov, JETP Lett., **111** (7), 376 (2020). DOI: 10.1134/S0021364020070085.
[2] J. Maser, G.B. Stephenson, S. Vogt, W. Yun, A. Macrander, H.C. Kang, C. Liu, R. Conley, Proc. SPIE, **5539**, 185 (2004). DOI: 10.1117/12.560046
[3] H.N. Chapman, C. Li, S. Bajt, M. Butola, J.L. Dresselhaus, D. Egorov, H. Fleckenstein, N. Ivanov, A. Kiene, B. Klopprogge, V. Kremling, P. Middendorf, D. Oberthuer, M. Prasciolu, T.E.S. Scheer, J. Sprenger, J.C. Wong, O. Yefanov, M. Zakharova, W. Zhang, Struct. Dyn., **12**, 014301 (2025). DOI: 10.1063/4.0000275

[4] J.L. Dresselhaus, H. Fleckenstein, M. Domaracky, M. Prasciolu, N. Ivanov, J. Carnis, K.T. Murray, A.J. Morgan, H.N. Chapman, S. Bajt, Rev. Sci. Instrum., **93**, 073704 (2022). DOI: 10.1063/5.0092269
[5] V.I. Punegov, Izv. Komi Nauchn. Tsentra Ural. Otd. Ross. Akad. Nauk. Ser. Fiz.-Mat. Nauki, No. 4 (44), 68 (2020) (in Russian). DOI: 10.19110/1994-5655-2020-4-68-73
[6] V.I. Punegov, J. Synchrotron. Rad., **28**, 1466 (2021). DOI: 10.1107/S1600577521006408
[7] V.I. Punegov, K.M. Pavlov, A.V. Karpov, N.N. Faleev, J. Appl. Cryst., **50**, 1256 (2017). DOI: 10.1107/S1600576717010123
[8] V.I. Punegov, J. Phys.: Conf. Ser., **2103**, 012145 (2021). DOI: 10.1088/1742-6596/2103/1/012145
[9] V.G. Kohn, I. Snigireva, A. Snigirev, Phys. Status Solidi B, **222**, 407 (2000). DOI: 10.1002/1521-3951(200011)222:2¡407
[10] A.V. Vinogradov, B.Ya. Zeldovich, Appl. Opt., **16**, 89 (1977). DOI: 10.1364/AO.16.000089
[11] S. Takagi, Acta Cryst., **15**, 1311 (1962). DOI: 10.1107/S0365110X62003473
[12] V.I. Punegov, S.I. Kolosov, K.M. Pavlov, Acta Cryst. A, **70**, 64 (2014). DOI: 10.1107/S2053273313030416

*Translated by D.Safin*